# A small lytic polysaccharide monooxygenase from *Streptomyces griseus* targeting α-and β-chitin

Yuko S. Nakagawa[a*], Madoka Kudo[a], Jennifer S. M. Loose[b], Takahiro Ishikawa[a], Kazuhide Totani[a], Vincent G. H. Eijsink[b] and Gustav Vaaje-Kolstad[b*]

[a] Department of Chemical Engineering, National Institute of Technology, Ichinoseki College, Ichinoseki 021-8511, Japan

[b] Department of Chemistry, Biotechnology and Food Science, Norwegian University of Life Sciences, Post Office Box 5003, 1432 Ås, Norway

*Corresponding authors

Tel: +81-191-24-4835; Fax: +81-191-24-2146

E-mail:gustav.vaaje-kolstad@nmbu.no or ynakagawa@ichinoseki.ac.jp

Running title: Characterization of a small LPMO from *Streptomyces griseus*

Abbreviations: LPMO: lytic polysaccharide monooxygenase, AA10: family 10 of the auxiliary activites, GlcNAc: *N*-acetyl-D-glucosamine, GlcNAc1A: *N*-acetyl-D-glucosaminic acid.

Keywords: AA10, LPMO, *Streptomyces griseus*, Chitinase, Chitin

ABSTRACT

The lytic polysaccharide monooxygenases (LPMOs) have received considerable attention after their discovery in 2010 due to their ability to boost the enzymatic conversion of recalcitrant polysaccharides. Here, we describe the enzymatic properties of *Sg*LPMO10F, a small (15 kDa) auxilliary activity family 10 (AA10) LPMO from *Streptomyces griseus* belonging to a clade of the phylogenetic tree without any characterized representative. The protein was expressed using a *Brevibacillus*-based expression system that had not been used previously for LPMO expression and that ensures correct processing of the N-terminus that is crucial for LPMO activity. The enzyme was active towards both α- and β-chitin and showed stronger binding and more release of soluble oxidized products for the latter allomorph. In chitinase synergy assays, however, *Sg*LPMO10F worked slightly better for α-chitin, increasing chitin solubilization yields up to ~30-fold and ~20-fold for α- and β-chitin, respectively. Synergy experiments with various chitinases showed that addition of *Sg*LPMO10F leads to a substantial increase in the $(GlcNAc)_2$:GlcNAc product ratio, in reactions with α-chitin only. This underpins the structural differences between the substrates and also shows that, on α-chitin, *Sg*LPMO10F affects the binding mode and/or degree of processivity of the chitinases tested. Variation in the only exposed aromatic residue in the substrate-binding surface of LPMO10s has previously been linked to preferential binding for α-chitin (exposed Trp) or β-chitin (exposed Tyr). Mutation of this residue, Tyr56, in *Sg*LPMO10F to Trp had no detectable effect on substrate binding preferences, but in synergy experiments the mutant seemed more efficient on α-chitin.

## INTRODUCTION

Chitin, a linear polysaccharide composed of GlcNAc units covalently connected by β-1, 4 linkages, is a highly abundant biomass present in crustacean and insect shells, as well as fungal cell walls. It is synthesized in Nature at a rate of $10^{11}$ tons per year [1]. When synthesized, chitin chains associate to form a crystalline structure that exists in two allomorphous forms, α (antiparallel chains) and β (parallel chains) [2, 3]. The recalcitrant nature of chitin complicates enzymatic degradation, but microorganisms have adapted to the challenge by developing efficient enzymatic systems. Often, such systems contain endo-type, non-processive chitinases that attack the amorphous parts of the substrate and exo-type processive chitinases that depolymerize the more crystalline regions of the chitin [4]. In addition to the hydrolytic activities provided by the chitinases, cleavage of chitin chains is also achieved by lytic polysaccharide monooxygenases (LPMOs; [5, 6]). LPMOs are thought to contribute to the efficiency of the degradative machinery by cleaving chitin chains in crystalline parts of the substrate that are inaccessible for the chitinases. Enzymes having this activity are classified in family 9, 10, 11 and 13 of the auxiliary activities (AA9, AA10, AA11 and AA13, respectively) in the Carbohydrate Active Enzymes database (CAZy; [7]). Whereas AA9-, AA11-, and AA13-type LPMOs (LPMO9s, LPMO11s and LPMO13s respectively) only have been identified in fungi, AA10-type LPMOs (LPMO10s) have been identified in eukaryotes, prokaryotes and viruses. LPMOs are known to target the crystalline surfaces of recalcitrant polysaccharides like chitin and cellulose, and cleave the glycosidic bonds of polysaccharide chains in their crystalline context through an oxidative mechanism [5, 8-13]. Recently, additional LPMO substrates have been discovered, including xyloglucan [14] and starch [15].

The LPMO active site contains two conserved histidines that bind a copper ion in a T-shaped histidine brace [9, 12, 16-19]. The copper ion is essential for catalysis and is thought to activate dioxygen through a redox cycle, eventually leading to hydroxylation of a glycosidic carbon (C1 or C4) and subsequent cleavage of the glycosidic bond through an elimination reaction [8, 11]. The reaction requires a supply of external electrons provided by small molecule reducing agents or protein donors [5, 8, 20]. Binding of LPMOs to their substrate is mediated by conserved amino acids on the flat surface of the enzyme that also accommodates the active site [19, 21]. LPMO10s are special in that they contain only one solvent exposed aromatic amino acid that is involved in substrate binding [6, 10, 16, 18, 19, 21, 22]. LPMO9s contain up to three solvent exposed aromatic amino acids on the binding surface [9, 23, 24]. LPMO10s have been shown to cleave both chitin and cellulose [5, 6, 12, 16, 25, 26]. All LPMOs so far characterized target insoluble polysaccharides, except for one LPMO9, *Nc*LPMO9C, which recently was shown to cleave soluble substrates like β-glucans [14, 27]. Under optimal conditions, the overall rate of enzymatic biomass hydrolysis can be increased by the presence of LPMOs and synergies between LPMOs and glycoside hydrolases are well documented for enzymatic solubilization of chitin [5, 6, 22, 28, 29]. In conclusion, available data indicate that LPMOs play important roles in the degradation of recalcitrant polysaccharides, a notion also supported by their abundant presence in the secretomes of biomass degrading microorganisms [30-33].

Members of the *Streptomyces* genus are important microbial contributors to biomass deconstruction in soil. These actinomycetes are known for their ability to degrade a variety of complex and recalcitrant polysaccharides [34], a property reflected by the abundance of carbohydrate active enzymes encoded in their genomes. In terms of chitin degradation, *Streptomyces* genomes sequenced show up to 11 putative chitinases belonging to family 18 of the glycoside hydrolases (GH18) and up to 4 putative GH20 chitobiases. Some species also have up to 6 putative GH19 chitinases. Furthermore, all sequenced species harbor multiple LPMO10s (except *S. cattleya* that only contains one). The involvement of *Streptomyces* LPMOs in biomass conversion was recently suggested by a comprehensive study on the transcriptome and secretome of *S. Sirex*AA-E [32]. Of the six LPMOs encoded by the *S. Sirex*AA-E genome, SACTE_0080, SACTE_2313, SACTE_6493 were highly expressed and secreted during growth on chitin, whereas SACTE_3159, SACTE_6428, SACTE_2313 were detected (in substantial amounts) during growth on cellulose. Oxidative degradation of cellulose has indeed be demonstrated for close homologues of SACTE_3159 and SACTE_6428, namely *Sc*LPMO10C (also called CelS2) and *Sc*LPMO10B from *S. coelicolor*, respectively [12, 16, 25].

Not much is known about the activity of putative chitin-active LPMOs from the *Streptomyces* genus, except substrate binding abilities. Both *S. reticuli* and *S. olivaceoviridis* secrete specific α-chitin binding putative LPMOs (CHB2 and CHB1, respectively; [35, 36]), where the former protein also has been shown to mediate contact between fungal and *Streptomyces* hyphae. CHB3 from *S. coelicolor* has been shown to bind to a variety of putative substrates, including α-chitin, β-chitin and chitosan [37].

In this study, we have analyzed a chitin-targeting LPMO from *S. griseus* HUT 6037, namely *Sg*LPMO10F. This LPMO represents an uncharacterized subclade of LPMO10s (Fig. 1) that is characterized by their small size and affiliation to the Actinomycetes phylum. The pure, recombinant wild type enzyme and a binding surface mutant were produced using a *Brevibacillus* -based expression method not previously described for LPMO production and the recombinant enzymes have been characterized with respect to oxidative activity and the ability to boost chitin hydrolysis by chitinases. We also describe and discuss how LPMO action is influenced by the differences between α- and β-chitin.

## RESULTS

Most genomes of biomass degrading bacteria only harbor one or two LPMO encoding genes, but the *Streptomyces* are an exception having up to seven (*S. coelicolor*). Until now only cellulose targeting LPMO10s from *Streptomyces* have been characterized [12, 16, 25]. The *S. griseus* genome contains six LPMO10-encoding genes that phylogenetically cluster with cellulose- or chitin-targeting LPMO10 sequences (Fig. 1 and Table 1; all *S. griseus* proteins were renamed according to the CAZy nomenclature; SGR_199: *Sg*LPMO10A, SGR_2956: *Sg*LPMO10B, SGR_4707: *Sg*LPMO10C, SGR_4740: *Sg*LPMO10D, SGR_5773: *Sg*LPMO10E and SGR_6855: *Sg*LPMO10F).

The small (15 kDa) LPMO, *Sg*LPMO10F, from the uncharacterized 1C subclade was chosen for further analysis. *Sg*LPMO10F is a low MW LPMO (only 15 kDa, 141 residues) and shares only 47% sequence identity with the closest characterized homologue, CBP21 (197 residues). A homology model of the *Sg*LPMO10F structure revealed a flat substrate-binding surface containing only one fully solvent exposed aromatic amino acid (Y56; Fig. 2A). Comparison with CBP21, the hitherto best characterized chitin-active LPMO10, shows that residues in the active site and substrate binding surface are conserved (Fig. 2A&B). The size difference between the two enzymes seems to result from two deletions in non-conserved loop regions on the "side" of protein (when regarding the substrate binding surface as "top"; Fig. 2).

*Sg*LPMO10F was expressed recombinantly in *B. choshinensis* SP3 using a method that ensures correct N-terminal processing. The protein was purified to ~95% purity by chitin affinity and gel filtration chromatography (Fig. 3A) and the average yield obtained was 2.5 mg pure protein per L culture.

For evaluation of the role of the only solvent exposed aromatic amino acid (Y56) on the substrate binding surface, this residue was mutated to a tryptophan. Substrate binding experiments showed that the wild-type and mutant enzyme have similar binding properties and that both bind stronger to β-chitin than to α-chitin (Fig. 3B).

*Sg*LPMO10F showed activity towards both chitin allomorphs, although only minor amounts of products were released from α-chitin particles (Fig. 4A). The oxidized chitooligosaccharides generated by *Sg*LPMO10F showed an elution profile and masses compatible with oxidation of the C1 carbon that leads to formation of aldonic acids (Fig. 4 A&B). The soluble products generated from β-chitin were dominated by the tetrameric and hexameric aldonic acids (Fig. 4; DP4ox and DP6ox, respectively).

Combination of the *S. marcescens* GH18 chitinases and *Sg*LPMO10F increased the solubilization rate of both chitin allomorphs (Fig. 5). Quantification of the effects is difficult because of non-linear progress curves, but enzyme-dependent differences in the synergistic effects are visible. Based on solubilization after 24 hours, addition of *Sg*LPMO10F increased α-chitin solubilization 9-, 29- and 23-fold for ChiA, ChiB and ChiC, while for β-chitin solubilization was increased 6-, 17- and 19-fold, respectively (Fig. 5 E&G). The maximum conversion yield obtained after 24h incubation was calculated to be 8% (obtained by ChiA+*Sg*LPMO10F) and 85% (obtained by ChiC+*Sg*LPMO10F)

for α- and β-chitin, respectively. The yield calculations included both GlcNAc and $(GlcNAc)_2$, which are by far the dominating products. Nevertheless, since chitooligosaccharide aldonic acids (not detectable in the HPLC method used) were not included, the maximum conversion yields are slightly underestimated.

Quantification of both major products resulting from chitin hydrolysis (GlcNAc and $(GlcNAc)_2$) enabled monitoring of the $(GlcNAc)_2$:GlcNAc ratio (dimer:monomer ratio; D:M), an indirect measure of chitinase processivity. For α-chitin solubilization, the D:M ratio was substantially higher for reactions containing *Sg*LPMO10F (Fig. 5F). For the same substrate, ChiA showed a higher D:M ratio than ChiB and ChiC in the absence of the LPMO. For β-chitin, D:M ratios were essentially identical for all chitinases, both in the presence and absence of *Sg*LPMO10F (Fig. 5H). Comparison of the two substrates show that the presence of the LPMO yields a D:M ratio for α-chitin that is in the range of what is observed for the solubilization of β-chitin.

Finally, the functional consequence of mutating Tyr56 to Trp was evaluated in synergy assays. In experiments repeated multiple times, the *Sg*LPMO10F_Y56W mutant showed a positive effect on the overall solubilization of α-chitin, and a negative effect on depolymerization of β-chitin compared to the WT enzyme (Fig. 6). For α-chitin solubilization, the reaction containing the WT enzyme is most efficient the first 24 hours, whereas the reaction containing the Y56W mutant maintains a steady rate and yields more products in the later stage of the reaction. For β-chitin, both variants perform similarly over the whole time range, with the wild-type being slightly more effective.

## DISCUSSION

A recent phylogenetic study on LPMO10 sequences reported two main clades (representing chitin- and cellulose-active LPMOs) that each include two subclades ([38] and Fig. 1). Closer inspection of subclades A and C opens for an even finer subclassification; subclade C can be divided into small- (~15 kDa) and medium- (~20 kDa) sized enzymes whereas subclade A can be divided into putatively membrane associated or free enzymes (Fig. 1). Interestingly, it has been shown that the *S. sp. sirex*AA-E LPMO in the membrane associated cluster (*Ss*LPMO10E; Fig. 1) is not upregulated on either cellulose or chitin [38]. Subclade C is dominated by actinobacterial enzymes that have not been biochemically characterized. In order to increase our understanding of LPMO function and also chitin degradation by *Streptomyces*, *Sg*LPMO10F was chosen for expression, purification and in-depth characterization.

When expressing LPMOs it is crucial to have no non-native amino acids on the N-terminus of the mature protein because both the primary amino group and the side chain of the N-terminal histidine found in all mature LPMOs are essential for coordination of the active site copper ion [18]. Thus, N-terminal affinity tags cannot be used unless the tag can be cleaved off by a protease that leaves no non-native amino acids on the mature protein (e.g. Factor Xa or Enterokinase). Such a strategy is laborious and final yields are often low. A more convenient and frequently used strategy for expression of bacterial LPMOs in *E. coli* is including a signal peptide for export of the recombinant protein into the periplasm. This paper describes the use of a Gram-positive expression system where the target protein is exported to the culture medium. Using this strategy, we were able to produce active *Sg*LPMO10F in amounts comparable to those obtained previously with *E. coli* expression systems in our laboratory.

The *Sg*LPMO10F sequence clusters with the main clade containing chitin active LPMO10s (Fig 1; clade I). A recent study by Takasuka *et al.* [32] showed that the transcript level for the *S. sirex* *Sg*LPMO10F homologue, *Ss*LPMO10A (Genebank ID: AEN08037.1; 79% identical to *Sg*LPMO10F), was increased 3.2-fold when the bacterium was grown on chitin compared to glucose as a carbon source indicating that the enzyme is active towards chitin. Indeed, binding assays, activity assays and chitinase synergy experiments with the recombinantly produced enzyme showed that both α- and β-chitin are substrates for the enzyme (Figs 3, 4 and 5, respectively). Comparison of *Sg*LPMO10F with a well characterized LPMO representing the I-D clade, CBP21 (referred to as "*Sm*LPMO10A" in Fig. 1), showed that they share conserved residues on the substrate binding surface (Fig 2.), indicating similar substrate preferences. CBP21 has previously been shown to bind strongly to β-chitin, but hardly to α-chitin [21, 31]. Despite the apparent similarity to CBP21, *Sg*LPMO10F binds relatively well to both chitin allomorphs (Fig. 3), indicating that additional structural features of the enzyme must play a role in binding.

A general characteristic of LPMO10 substrate-binding surfaces is the presence of a single [19, 21] solvent exposed, aromatic amino acid. This residue has previously been shown to play an important role in substrate binding; CBP21 has a Tyr in this position and mutation of this residue to Ala reduces binding to β-chitin [21]. CHB2 and CHB1 from *S. reticuli* and *S. olivaceoviridis*, respectively have a Trp in this position and bind better to α-chitin than β-chitin [35, 36]. A mutagenesis study of CHB1

showed reduction in substrate binding when the solvent exposed tryptophan (Trp57) was mutated to tyrosine [36]. These observations could indicate that the Tyr/Trp variation is a determinant of allomorph binding specificity, but recent data indicate otherwise: *Ef*CBM33A, an LPMO from *E. faecalis* has a tryptophan as the only solvent exposed aromatic amino acid (Trp58) and has approximately equal binding preferences for α-and β-chitin [6]. To address this issue, Tyr56 in *Sg*LPMO10F was mutated to tryptophan and substrate binding properties were evaluated. The binding data show that the mutation has no effect on the β-chitin binding and only a minor effect on α-chitin binding. Thus, when it comes to binding as such, additional structural features of the enzyme must play a role, for example the network of mainly polar side chains that protrude from the binding surface (Fig. 2). In this context, it should be noted that observed binding abilities of LPMO10s may be deceptive. For example, the catalytic LPMO10 module of *Sc*LPMO10C (CelS2) from *S. coelicolor* binds strongly to both α- and β-chitin, but is only active on cellulose [12]. Also, CBP21 binds only weakly to α-chitin but is nevertheless capable of cleaving the glycosidic bonds of this substrate and to contribute to the overall efficiency of its degradation [39]. Activity data and the possible role of the exposed aromatic residue are discussed further below.

The product profile generated by *Sg*LPMO10F shows a dominance of even numbered products, which is commonly observed for both chitin and C1- oxidizing cellulose-active LPMO10s [5, 13, 16, 25, 41]. As previously discussed by Vaaje-Kolstad *et al*. [5], the dominance of even numbered products is most likely a consequence of the LPMO cleaving polysaccharide chains embedded in a crystalline matrix. The two-fold screw axis of the chitin/cellulose chain will only allow productive binding to every second monosaccharide in the polymer chain. This will yield a dominance of even numbered soluble products. The product profiles also show that longer chitooligosaccharides are released from β-chitin than α-chitin. A possible explanation is that the tighter packing of the chitin chains of α-chitin compared to β-chitin gives less efficient solubilization of the former substrate

One of the most prominent properties of LPMOs is their ability to boost the activity of glycoside hydrolases in biomass solubilization reactions. *Sg*LPMO10F does indeed have a major impact on the solubilization of both α- and β-chitin by chitinases, increasing solubilization rates and increasing 24-hour solubilization yields by up to 29- and 19-fold for α- and β-chitin respectively (Fig. 5). Previous studies on LPMO-GH synergies have shown that LPMOs can increase substrate solubilization yields from ~1.5- to 10-fold [5, 6, 8, 22, 25, 28, 29, 39-41]. A direct comparison of these data to the results obtained in this study is problematic due to the wide range of substrate concentrations (0.1 to 4.0 mg/mL) and other experimental conditions used. Using almost similar conditions as in the present study, Nakagawa et al. showed that CBP21 only had a modest effect on the conversion efficiency of crystalline α-chitin, with yield increases ranging from < 1.5 fold for ChiA and ChiC to 5-fold for ChiB [39]. I thus seems that *Sg*LPMO10F is better tuned to α -chitin depolymerization than CBP21. As a matter of fact, *Sg*LPMO10F appears to be more important for α-chitin degradation than for β-chitin degradation, despite the low apparent LPMO activity on the former substrate (Fig. 4A). Considering the complexity, heterogeneity and recalcitrance of the

substrate, there are conceivable scenarios that could explain the observations made for α-chitin. For example, the LMPO could act on regions of the substrate that only become available after chitinase action. Alternatively, one difference between α-chitin and β-chitin could be the presence of obstacles in the former substrate at which chitinases may stall [42-44]. Specific LPMO activity in obstacle-rich regions could be crucial in synergy experiments (Fig. 5), while having relatively marginal effects on the release of soluble products (Fig. 4).

Although the effect of *Sg*LPMO10F was highest in α-chitin solubilization, overall, the enzymatic degradation process was most effective for β-chitin for all enzyme combinations, as observed previously [39]. These results highlight the higher degree of recalcitrance of α-chitin compared to β-chitin. Furthermore, whereas degradation of β-chitin seems to continue with an approximately constant rate within the time frame of the experiment, α-chitin depolymerization slows down after 8 h. The gradual decrease in solubilization rate, which is commonly observed in reactions involving crystalline substrates such as chitin or cellulose, has been suggested to arise from immobilization of the enzymes on the substrate surface, as alluded to above [42, 43]. Notably, previous studies suggest that the slowing down of reactions with α-chitin can partially be circumvented by mechanical pretreatment prior to enzymatic conversion [39].

Interestingly, the Y56W mutation had a positive effect on the ability of *Sg*LPMO10F to increase the yield of α-chitin degradation by ChiC. While in reactions with the wild-type enzyme the reaction slows down after 24h, the reaction proceeds with constant speed in the presence of the mutant (Fig. 6A). This effect is not observed for β-chitin, where the mutant seems to perform slightly less well than the wild type (Fig. 6B). The binding assays of Fig. 3 show that the change in activity cannot be directly related to the binding properties of the enzyme, in line with previous observations on a lack of correlation between binding preferences and catalytic substrate specificity (discussed above). It is thus likely that the mutation affects the geometry of binding, including the positioning of the catalytic site relative to glycosidic bond targeted for oxidation. It is interesting to note that the present data confirm a correlation between the presence of Trp as exposed aromatic residue and activity on α-chitin, which was originally proposed on the basis of binding data only [36].

For both substrates, the effect of *Sg*LPMO10F was least for ChiA, the most powerful of the chitinases when applied alone, whereas effects on ChiB and ChiC were higher and similar (Fig. 5). Since ChiC is a non-processive chitinase thought to act on amorphous parts of the substrate [4], it can be envisioned that a crystal-surface disrupting activity of *Sg*LPMO10F has a particularly large effect on this enzyme. Indeed, using rather extreme experimental conditions promoting maximal activity, it has been shown that CBP21 can render crystalline β-chitin amorphous [5]. The difference between ChiA and ChiB, both processive chitobiohydrolases working in opposite directions [4, 45, 46] is more difficult to explain. Several papers [39, 47, 48] as well as unpublished observations from our laboratory, show that ChiA generally is a more powerful enzyme, which in itself could explain the more modest effect of combining with additional enzymes such as *Sg*LPMO10F. It is also possible

that the difference in the CBMs of the two chitinases leads to different binding abilities and binding geometries that are differentially affected by *Sg*LPMO10F. Finally, *Sg*LPMO10F, leaves C1 oxidized chain ends at the cleavage site ("oxidized reducing ends") which may affect ChiA, working from the non-reducing end, and ChiB, working from the reducing end, in different ways.

The influence of LPMOs on the processivity of glycoside hydrolases has hitherto not been studied and the calculation of the D:M ratio for the LPMO-chitinase synergy experiments allowed insight into this property. A highly processive enzymes usually gives a high D:M ratio, whereas the opposite is observed for non-processive enzymes [49]. It should be noted that some caution is needed when interpreting these ratios since this parameter in part also reflects the binding preferences of the enzymes to both the polymer chains and intermediate oligomeric products [50]. The most striking feature of the D:M plots is the elevated D:M ratios observed for α-chitin degradation caused by *Sg*LPMO10F activity (Fig. 5F). The same trend is not observed for β-chitin degradation. On the contrary, the D:M ratio seems rather to be lowered or not changed at all by the presence of *Sg*LPMO10F (Fig. 5H). A likely explanation for processive ChiA and ChiB would be that *Sg*LPMO10F removes "obstacles", be it regions of high crystallinity or otherwise inaccessible regions that limit the degree of processivity. The existence of such obstacles and their impact on enzyme efficiency and processivity have been discussed extensively for cellulases [42-44, 51], but possible roles of LPMOs in removing them have not yet been assessed. The presence of obstacles where the processive chitinases ChiA and ChiB could stall is much more likely for α-chitin than for β-chitin, with its more loosely packed structure [2]. The situation is less clear for the endochitinase ChiC, which, notably, tends to predominantly produce dimers from chitin despite its lack of processivity [48, 50]. Perhaps, in the absence of *Sg*LPMO10F, ChiC primarily attacks the amorphous "easily accessible" parts of the substrate, perhaps even with a bias for (protruding) chain ends, which would result in relatively high production of odd-numbered intermediate products and thus, a low D:M ratio. The presence of *Sg*LPMO10F could increase the accessibility of the more ordered, crystalline parts of the substrate, which will lead to higher production of even numbered products, for the same reasons as those underlying the product profiles of *Sg*LPMO10F (Fig. 4), discussed above. Further work is needed to verify these possible explanations. However, the present results demonstrate that the effect of an LPMO is clearly affected by the structure of the substrate. Turning this around, and considering the different co-polymeric structures in which chitin occurs in nature (e.g. fungal cell walls, insect shells), organisms may need several LPMOs to optimally harvest from available chitin resources, as is indeed observed in the genomes of many microbes.

In conclusion, the present data show that the small LPMO, *Sg*LPMO10F, clustering in the hitherto not studied Clade IC of Figure 1, is a chitin-active enzyme that can contribute to the enzymatic conversion of various chitin forms. The qualitative and quantitative impact of this LPMO depends on the substrate and the only exposed aromatic residue in LPMO10s seems to be one determinant of this impact. Many questions related to enzyme kinetics, optimization of the interplay between LPMOs and chitinases, and the structural determinants of binding and substrate specificity remain for

*Sg*LPMO10F and, in fact, all other LPMOs. Due to the importance of LPMOs in biomass conversion, these enzymes are currently the subject of many studies, which hopefully will shed more light on these issues.

## MATERIALS AND METHODS

### *Cloning of* Sg*LPMO10F*

The *S. griseus subsp. griseus* NBRC3237 strain was obtained from the Biological Resource Center (NBRC) and genomic DNA was obtained from bacterial cells arising from a single colony grown over night on a Yeast extract-starch agar plate. The cells were harvested with a sterile toothpick, transferred to a sterile 1.5 mL test tube and mixed thoroughly with 20 µl Lyse-and-Go PCR reagent (Thermo Scientific). The lysed cells were immediately centrifuged for 1 minute at 12900 xg and the supernatant (containing genomic DNA) was stored at -20°C until use. Cloning of the *gene* encoding *Sg*LPMO10F (WP_003971177) was accomplished by PCR using the bacterial lysate as template source and cloning primers designed to not include the signal peptide. The primer sequences were: forward: 5'-CAACCTCTACATCGGCACTCGCTTTCGGTACCCTC-3' and reverse: 5'-AGCTGCAGTTGCAGCCGATCTTCGAAGCCGTAATA -3'as a reverse primer. The In-Fusion HD cloning kit (Clontech) was used to ligate the amplified fragment into the pNCMO2 (Takara) expression vector in frame with a signal peptide encoding sequence that enables secrection of the target protein when using *Brevibacillus choshinensis* as a production strain. Upon secretion, the signal peptide is cleaved off yielding a protein product with no non-native amino acids on the N-terminus of the mature protein. This is vital when expressing LPMOs since the amino group of the N-terminal amino acid (a histidine) is essential for enzyme activity. The sequence of the DNA inserted was confirmed by sequencing.

### *Site directed mutagenesis*

Change of the codon for Tyr56 to a codon encoding tryptophan was accomplished by site directed mutagenesis using the Prime STAR Mutagenesis Basal Kit (Takara) using the following primers, forward: 5'-ATCAAGTGGGAACCGCAGAGCGTCGAG-3' and reverse: 5'-CGGTTCCCACTTGATCGCACCGCAGCT-3'. The sequence of the altered DNA was confirmed by sequencing.

### *Recombinant protein expression and purification*

The pNCMO2 vectors containing the genes encoding *Sg*LPMO10F, α-amylase (positive control) or no insert (negative control) were transformed into *Brevibacillus choshinensis* SP3 (Takara) followed by cultivation for 24 h at 30ºC in 2SY broth containing 50 µg/ml neomycin. After cultivation, the culture was centrifuged at 10600 x g for pelleting the bacteria. Subsequently, the proteins in the supernatant were concentrated 12-fold by ultrafiltration using a Vivaflow200 apparatus (Sartorius) with a 10 kDa cutoff filter cassette.

Recombinant *Sg*LPMO10F was purified by chitin affinity chromatography using the method of Vaaje-Kolstad *et al.* [21] followed by gel filtration chromatography using Superose 12 10/300 GL (GE Healthcare) operated in an ÄKTA Explorer system (GE Healthcare). The running buffer contained 20 mM Tris-HCl pH 8.0 and 150 mM NaCl and the flow rate was 0.5 ml/min. Eluted protein fractions containing *Sg*LPMO10F were pooled and concentrated by ultrafiltration using

Amicon Ultra 15 centrifugal devices with 10 kDa cut-off (Merck Millipore), followed by sterile filtering and storage at 4ºC until use. Protein concentration was measured using the Coomassie Protein Assay Kit (Thermo Scientific) and purity was assessed by SDS-polyacrylamide gel electrophoresis (SDS-PAGE).

ChiA, -B and -C from *S. marcescens* were expressed in purified as previously described [52-54]. All enzymes were purified by chitin affinity chromatography using the protocol developed for CBP21 [21]. In short, periplasmic extracts of *E. coli* cultures containing the enzyme of interest prepared by cold osmotic shock according to [53], were passed through a 20 ml chitin bead (New England Biolabs) column equilibrated with 20 mM Tris-HCl pH 8.0. Bound enzymes were eluted by application of 20 mM acetic acid. Fractions containing eluted enzyme were adjusted to pH 8.0 immediately after collection by addition of 1.0 M Tris-HCl pH 8.0 in small volumes until the target pH was reached. Finally the fractions were concentrated with Vivaspin ultrafiltration devices (Sartorius), followed by buffer change to 20 mM Tris-HCl pH 8.0 using the same device. All enzymes were kept at 4°C until use.

*Chitin binding assay*

Binding of *Sg*LPMO10F WT and Y56W to chitin was assayed using shrimp shell α-chitin powder (Hov Bio, Tromsø, Norway) or squid pen β-chitin powder (France chitin, Orange, France) as substrates. Reaction mixtures were composed by mixing 1.0 mg substrate with 100 µl enzyme solution containing 10 µM LPMO in 50 mM ammonium acetate, pH 6.3 (binding buffer). The mixture was incubated statically for 3 h at 37°C, followed by centrifugation for 1 minute at 2100 x g. Both the supernatant (containing protein not bound to chitin) and the chitin pellet (containing protein bound to chitin) were collected and mixed with an equal volume or 20 µl of SDS-PAGE sample buffer, respectively. Both samples were mixed thoroughly and boiled for 10 minutes before centrifugation and subsequent analysis of 10 µl sample with SDS-PAGE. The combination of SDS-PAGE buffer and incubation at high temperature desorbs all proteins bound to the chitin particles. The SDS-PAGE gel was stained with Coomassie Brilliant Blue G250 and densiometric quantification of the protein bands was performed using the ImageJ software (National Institute of Health).

*Enzyme assays*

Enzyme assays for determining *Sg*LPMO10F-chitinase synergies were done as follows. Reaction mixtures (500 µl) contained 4 mg/ml α-chitin (Hov-Bio) or β-chitin (France Chitin) as substrates, 0.2-1.5 µM chitinase (ChiA, B or C) and 1.0 mM ascorbic acid in 50 mM ammonium acetate buffer pH 6.3, in the presence or absence of 1.0 µM *Sg*LPMO10F. Reactions were incubated statically at 37°C. Enzyme reaction aliquots (60 µl) were collected at time points ranging from 2 to 24 hours and enzyme activity was terminated by addition of 60 µl 50 mM $H_2SO_4$. Before further analysis, undegraded chitin was removed from the samples by centrifugation at 12900 x g for 2 min and supernatants were collected. Quantities of GlcNAc and $(GlcNAc)_2$ were determined by high preassure liquid chromatography (HPLC) using a Shimadzu Prominence HPLC system equipped with a Rezex RFQ-Fast acid $H^+$ (8%) 7.8 x 100 mm (Phenomenex) column with a Carbo-H, 4 x 3.0 mm guard column and Rezex RFQ-Fast Acid $H^+$ (8%) 7.8 x 50 mm fitted in front. Separation of analytes was performed isocratically using a mobile phase composed of 5 mM $H_2SO_4$ running with a flow rate of 1.0 ml/min. Eluted GlcNAc and $(GlcNAc)_2$ were detected by monitoring absorbance at 195 nm. Calibration standards were run routinely. All reactions were run in triplicate. Enzyme assays conducted to compare the contribution of *Sg*LPMO10F_WT and *Sg*LPMO10F _Y56W to chitin hydrolysis by ChiC were performed and analyzed using the same conditions and methods as stated above, but using 4 mg/ml α-chitin from Yaizu Suisankagaku Industry Co. Ltd. (Shizuoka, Japan) and β-chitin from Seikagaku Kogyo (Tokyo, Japan) as substrates.

Enzyme assays for determination of *Sg*LPMO10F activity [i.e. release of chitooligosaccharide aldonic acids; $(GlcNAc)_nGlcNAc1A$], were conducted by incubating reaction mixtures (500 µl) containing 1.0 µM *Sg*LPMO10F, 1.0 mM ascorbic acid and 5 mg/ml β–chitin nanofibers in 50 mM Tris-HCl pH 8.0 at 40°C with shaking at 1000 rpm. β–chitin nanofibers were used because this substrate provides enhanced reproducibility and sensitivity relative to other substrates. The nanofibers were made by following the protocol previously published by Fan *et al*., i.e. by sonicating β-chitin (France Chitin) in an acidic solution (1.8 mM acetic acid; see [55] for details). After starting the enzymatic reactions samples were taken at 30 minute intervals and reactions were stopped by separating the insoluble substrate from soluble reactants and products by filtration using a 96-well filter plate (Millipore) operated by a Millipore vacuum manifold. The relative quantity of oxidized chitooligosaccharides in the samples was analyzed by UHPLC using the method previously described by Vaaje-Kolstad *et al.* [5], but with a slightly different gradient; 0-5 minutes (74% acetonitrile), 5-7 min (74%-62% acetonitrile), 7-8 min (62% acetonitrile), 8-10 min (62%-74% acetonitrile) and 10-12 min (74% acetonitrile). Standards were obtained by enzymatic oxidation of chitooligosaccharides (DP2-6) by chitooligocsaccharide oxidase (ChitO; [56]) according to the protocol described by Loose *et al.* [13].

To obtain product profiles reactions were carried out using the conditions described for the

*Sg*LPMO10F activity assay except that 10.0 mg/ml α- or β-chitin particles were used as substrate, instead of β-chitin nanofibers. Analysis of the resulting chitooligosaccharide aldonic acids was done by UPLC and MALDI-TOF MS as described previously by Vaaje-Kolstad *et al.* [5].

*Homology modeling*

A 3D-structural model of *Sg*LPMO10F was obtained by homology modeling using the SwissModel server [57]. The modeling procedure was performed using default parameters and the CBP21 X-ray crystallographic structure (PDB code 2BEM, chain A) as template structure.

ACKNOWLEDGMENTS

We thank Anne C. Bunæs, NMBU, for purification of recombinant proteins. This work was supported by Grant for a research worker in abroad from Institute of National College of Technology and Grant-in-Aid for Young Scientists (B) (#22780097 and #25850077) and Program for Revitalization Promotion, JST. GV-K and JSML were supported by the Norwegian Research Council (grant 214138).

FIGURE LEGENDS

**Figure 1. Phylogenetic clustering of LPMO10 sequences.** Representative enzymes sequences have been selected from the phylogenetic tree published by Book *et al.* [38] and re-clustered using Phylogeny.fr [58]. Only sequences of catalytic LPMO10 modules were used in the analysis. The presence of carbohydrate binding modules (CBMs) is indicated by the protein names. Enzymes that have been biochemically characterized in other studies are shown in blue colored bold text. The clades and sub-clades identified by Book *et al.* [38] are separated by a dashed black line and the subclades are labeled by circled bold letters. The *S. griseus* LPMO10 protein names are shown in bold formatting and black color, except the enzyme investigated in this study, which is colored pink. The Uniprot and/or Genbank identifiers of all sequences analyzed, as well as literature references for characterized LPMOs are provided in Table 1.

**Figure 2. Structural comparison of CBP21 and *Sg*LPMO10F.** The top panels show CBP21 (A) and *Sg*LPMO10F (B) in cartoon and transparent surface representation. Deletions in *Sg*LPMO10F are colored orange in CBP21. The bottom panels show the substrate binding surface of CBP21 and *Sg*LPMO10F, with the side chains of residues identified as important substrate binding and activity in CBP21 [19, 21, 22] shown in stick representation with magenta, blue and red colored carbon, oxygen and nitrogen atoms, respectively. Note that His28 and His31 are the N-terminal residues of the two proteins, respectively. (C) Structures of CBP21 and *Sg*LPMO10F shown in ribbon representation with selected side chains (active site histidines, a surface tyrosine and disulphide bonds) shown in stick representation. Disulphide bonds are shown in green color. The sequence identity between *Sg*LPMO10F and CBP21 is 47% and the Swiss-Model "estimated absolute model quality" of the *Sg*LPMO10F structure yielded a QMEAN4 score of -2.32.

**Figure 3. Production of *Sg*LPMO10F and evaluation of substrate binding properties.** (A) Expression and purification of *Sg*LPMO10F represented by SDS-PAGE analysis of the culture supernatant from a culture grown overnight (lane 2), purified protein after chitin-bead purification (lane 3) and fully purified *Sg*LPMO10F after subsequent SEC purification (lane 4). Lane 1 shows the protein molecular weight ladder. (B) Binding of 10 μM *Sg*LPMO10F WT or Y56W to 10 mg/ml α-chitin (Hov-Bio) or β-chitin (France Chitin) in 50 mM ammonium acetate buffer pH 6.3 assayed by analyzing protein in the liquid phase (non-bound; "NB") and protein bound to the chitin (bound; "B") by SDS-PAGE. Please note that the NB fractions are 5-fold diluted compared the B fractions. Based on densiometry using ImageJ, and after correcting for the dilution factors, the estimated fractions of bound protein under these conditions were approximately 16 % and 35% for WT *Sg*LPMO10F and 19 % and 35% for the Y56W mutant, for α- and β-chitin, respectively.

**Figure 4. Activity of *Sg*LPMO10F towards chitin.** (A) UPLC analysis of products generated by 1.0 μM *Sg*LPMO10F acting on 10.0 mg/ml β-chitin (France Chitin) or 10.0 mg/ml α-chitin (Hov-Bio) in the presence of 1.0 mM ascorbic acid, incubated for 150 minutes in 50 mM Tris pH 8 at 40°C. MALDI-TOF MS analysis of the β- and α-chitin samples shown in panel (A) are illustrated

in panels (B) and (C), respectively. Each aldonic acid chitooligosaccharide product is identified by one major peak that represents the mass of the [M+$Na^+$] adduct. Some products are also represented by peaks of lower intensity that represent masses of the [M+$K^+$], [M-$H^+$+2$Na^+$], [M-$H^+$+$K^+$+$Na^+$] and/or [M-$H^+$+2$K^+$] adducts. The masses observed for the [M+$Na^+$] adducts were 869.1 ($DP4_{ox}$), 1072.2 ($DP5_{ox}$), 1275.2 ($DP6_{ox}$), 1478.3 ($DP7_{ox}$) and 1681.4 ($DP8_{ox}$). $DPn_{ox}$ indicates the degree of polymerization (DP) of the C1 oxidized chitooligosaccharide (e.g. $DP6_{ox}$ refers to $(GlcNAc)_5$GlcNAc1A, where GlcNAc1A is the aldonic acid form of GlcNAc). (C) Relative quantification of products generated by 1.0 μM *Sg*LPMO10F acting on 5.0 mg/ml β-chitin nanofibers in 50 mM Tris-HCl, pH 8.0 in the presence of 1.0 mM ascorbic acid at 40°C by UPLC. The substrate used in this assay is the same as used in panel A, but the substrate was pretreated by sonication in order to disassemble the nanofibre aggregates in the β-chitin particles. This gives a more homogenous substrate that is better suited for kinetic experiments.

**Figure 5. Enzymatic solubilization of chitin.** Degradation of 4.0 mg/ml α-chitin or β-chitin by 0.2 μM *S. marcescens* chitinases (ChiA, ChiB or ChiC) in the presence or absence of 1.0 μM *Sg*LPMO10F in ammonium acetate buffer pH 6.3 at 37°C with 1.0 mM ascorbic acid included as electron donor in all reactions. Solubilization was determined by monitoring release of $(GlcNAc)_2$ (A&C) and GlcNAc (B&D). The error bars represent SD (n = 3). The data points from the first 8h of each progress curve are also shown separately (indicated by arrow) in order to give a clearer view of this phase of the reaction. Panels (E) and (G) indicate the increase in chitin hydrolysis observed at 24 h caused by the presence of *Sg*LPMO10F. The fold increase was calculated by dividing the sum of total soluble products (GlcNAc and $(GlcNAc)_2$) in GlcNAc equivalents (molar) obtained by individual chitinases in the presence of *Sg*LPMO10F by the sum of products generated by the individual chitinases in the absence of *Sg*LPMO10F. The $(GlcNAc)_2$:GlcNAc ratios for α- and β-chitin degradation are indicated in panels F and H, respectively. The β-chitin graph does not show data for ChiB because in several samples the GlcNAc concentrations were too low to be determined accurately.

**Figure 6. Degradation of chitin in the presence or absence of *Sg*LPMO10F WT or Y56W**. Hydrolysis of 4.0 mg/ml α-chitin (Yaegaki Bio-Industries Inc.) or β-chitin (Seikagaku Kogyo) by 0.2 μM ChiC in the presence or absence of 1.0 μM *Sg*LPMO10F WT or Y56W in 50 mM ammonium acetate buffer pH 6.3 at 37°C. The error bars represent SD (n = 3). Some SDs are too low to be observed (hidden by data symbols). Binding profiles of *Sg*LPMO10F WT and Y56W to this chitin powders were essentially identical to what was observed for the Hov-Bio α-chitin and France Chitin β-chitin shown in Figure 3 (results not shown). The lower solubilization yields obtained (compared to Figure 5) is most likely due to the larger particle size of the Yaegaki and Seikagaku chitin powders.

REFERENCES

1. Gooday, G. W. (1990) The ecology of chitin degradation. *Adv Microb Ecol* **11**, 387-430.

2. Blackwell, J. (1969) Structure of Beta-Chitin or Parallel Chain Systems of Poly-Beta-(1-4)-N-Acetyl-D-Glucosamine. *Biopolymers* **7**, 281-298.

3. Minke, R. & Blackwell, J. (1978) Structure of alpha-Chitin. *J Mol Biol* **120**, 167-181.

4. Vaaje-Kolstad, G., Horn, S. J., Sørlie, M. & Eijsink, V. G. H. (2013) The chitinolytic machinery of *Serratia marcescens* - a model system for enzymatic degradation of recalcitrant polysaccharides. *Febs J* **280**, 3028-3049

5. Vaaje-Kolstad, G., Westereng, B., Horn, S. J., Liu, Z. L., Zhai, H., Sørlie, M. & Eijsink, V. G. H. (2010) An oxidative enzyme boosting the enzymatic conversion of recalcitrant polysaccharides. *Science* **330**, 219-222.

6. Vaaje-Kolstad, G., Bøhle, L. A., Gåseidnes, S., Dalhus, B., Bjørås, M., Mathiesen, G. & Eijsink, V. G. H. (2012) Characterization of the chitinolytic machinery of *Enterococcus faecalis* v583 and high-resolution structure of its oxidative CBM33 enzyme. *J Mol Biol* **416**, 239-254.

7. Levasseur, A., Drula, E., Lombard, V., Coutinho, P. M. & Henrissat, B. (2013) Expansion of the enzymatic repertoire of the CAZy database to integrate auxiliary redox enzymes. *Biotechnol Biofuels* **6**, 41.

8. Phillips, C. M., Beeson, W. T., Cate, J. H. & Marletta, M. A. (2011) Cellobiose dehydrogenase and a copper-dependent polysaccharide monooxygenase potentiate cellulose degradation by *Neurospora crassa*. *ACS Chem Biol* **6**, 1399-1406.

9. Quinlan, R. J., Sweeney, M. D., Lo Leggio, L., Otten, H., Poulsen, J. C., Johansen, K. S., Krogh, K. B., Jorgensen, C. I., Tovborg, M., Anthonsen, A., Tryfona, T., Walter, C. P., Dupree, P., Xu, F., Davies, G. J. & Walton, P. H. (2011) Insights into the oxidative degradation of cellulose by a copper metalloenzyme that exploits biomass components. *Proc Natl Acad Sci U S A* **108**, 15079-15084.

10. Hemsworth, G. R., Davies, G. J. & Walton, P. H. (2013) Recent insights into copper-containing lytic polysaccharide mono-oxygenases. *Curr Opin Struct Biol* **23**, 660-668.

11. Kim, S., Ståhlberg, J., Sandgren, M., Paton, R. S. & Beckham, G. T. (2014) Quantum mechanical calculations suggest that lytic polysaccharide monooxygenases use a copper-oxyl, oxygen-rebound mechanism. *Proc Natl Acad Sci U S A* **111**, 149-154.

12. Forsberg, Z., Røhr, A. K., Mekasha, S., Andersson, K. K., Eijsink, V. G. H., Vaaje-Kolstad, G. & Sørlie, M. (2014) Comparative study of two chitin-active and two cellulose-active AA10-type lytic polysaccharide monooxygenases. *Biochemistry* **53**, 1647-1656.

13. Loose, J. S. M., Forsberg, Z., Fraaije, M. W., Eijsink, V. G. H. & Vaaje-Kolstad, G. (2014) A rapid quantitative activity assay shows that the *Vibrio cholerae* colonization factor GbpA is an active lytic polysaccharide monooxygenase. *FEBS Lett* **588**, 3435-3440.

14. Agger, J. W., Isaksen, T., Varnai, A., Vidal-Melgosa, S., Willats, W. G., Ludwig, R., Horn, S. J., Eijsink, V. G. H. & Westereng, B. (2014) Discovery of LPMO activity on hemicelluloses shows the importance of oxidative processes in plant cell wall degradation. *Proc Natl Acad Sci U S A* **111**, 6287-6292.

15. Vu, V. V., Beeson, W. T., Span, E. A., Farquhar, E. R. & Marletta, M. A. (2014) A family of starch-active polysaccharide monooxygenases. *Proc Natl Acad Sci U S A* **111**, 13822-7.

16. Forsberg, Z., Mackenzie, A. K., Sørlie, M., Røhr, A. K., Helland, R., Arvai, A. S., Vaaje-Kolstad, G. & Eijsink, V. G. H. (2014) Structural and functional characterization of a conserved pair of bacterial cellulose-oxidizing lytic polysaccharide monooxygenases. *Proc Natl Acad Sci U S A* **111**, 8446-8451.

17. Gudmundsson, M., Kim, S., Wu, M., Ishida, T., Momeni, M. H., Vaaje-Kolstad, G., Lundberg, D., Royant, A., Stahlberg, J., Eijsink, V. G. H., Beckham, G. T. & Sandgren, M. (2014) Structural and electronic snapshots during the transition from a Cu(II) to Cu(I) metal center of a lytic polysaccharide monooxygenase by X-ray photoreduction. *J Biol Chem* **289**, 18782-18792.

18. Hemsworth, G. R., Taylor, E. J., Kim, R. Q., Gregory, R. C., Lewis, S. J., Turkenburg, J. P., Parkin, A., Davies, G. J. & Walton, P. H. (2013) The copper active site of CBM33 polysaccharide oxygenases. *J Am Chem Soc* **135**, 6069-6077.

19. Aachmann, F. L., Sørlie, M., Skjåk-Bræk, G., Eijsink, V. G. H. & Vaaje-Kolstad, G. (2012) NMR structure of a lytic polysaccharide monooxygenase provides insight into copper binding, protein dynamics, and substrate interactions. *Proc Natl Acad Sci U S A* **109**, 18779-18784.

20. Langston, J. A., Shaghasi, T., Abbate, E., Xu, F., Vlasenko, E. & Sweeney, M. D. (2011) Oxidoreductive cellulose depolymerization by the enzymes cellobiose dehydrogenase and glycoside hydrolase 61. *Appl Environ Microbiol* **77**, 7007-7015.

21. Vaaje-Kolstad, G., Houston, D. R., Riemen, A. H. K., Eijsink, V. G. H. & van Aalten, D. M. F. (2005) Crystal structure and binding properties of the *Serratia marcescens* chitin-binding protein CBP21. *J Biol Chem* **280**, 11313-11319.

22. Vaaje-Kolstad, G., Horn, S. J., van Aalten, D. M. F., Synstad, B. & Eijsink, V. G. H. (2005) The non-catalytic chitin-binding protein CBP21 from *Serratia marcescens* is essential for chitin degradation. *J Biol Chem* **280**, 28492-28497.

23. Wu, M., Beckham, G. T., Larsson, A. M., Ishida, T., Kim, S., Payne, C. M., Himmel, M. E., Crowley, M. F., Horn, S. J., Westereng, B., Igarashi, K., Samejima, M., Stahlberg, J., Eijsink, V. G. H. & Sandgren, M. (2013) Crystal structure and computational characterization of the lytic polysaccharide monooxygenase GH61D from the Basidiomycota fungus *Phanerochaete chrysosporium*. *J Biol Chem* **288**, 12828-39.

24. Li, X., Beeson, W. T. t., Phillips, C. M., Marletta, M. A. & Cate, J. H. (2012) Structural basis for substrate targeting and catalysis by fungal polysaccharide monooxygenases. *Structure* **20**, 1051-1061.

25. Forsberg, Z., Vaaje-Kolstad, G., Westereng, B., Bunæs, A. C., Stenstrøm, Y., Mackenzie, A., Sørlie, M., Horn, S. J. & Eijsink, V. G. H. (2011) Cleavage of cellulose by a CBM33 protein. *Protein Sci* **20**, 1479-1483.

26. Horn, S. J., Vaaje-Kolstad, G., Westereng, B. & Eijsink, V. G. H. (2012) Novel enzymes for the degradation of cellulose. *Biotechnol Biofuels* **5**, 45.

27. Isaksen, T., Westereng, B., Aachmann, F. L., Agger, J. W., Kracher, D., Kittl, R., Ludwig, R., Haltrich, D., Eijsink, V. G. H. & Horn, S. J. (2014) A C4-oxidizing lytic polysaccharide monooxygenase cleaving both cellulose and cello-oligosaccharides. *J Biol Chem* **289**, 2632-2642.
28. Purushotham, P., Arun, P. V., Prakash, J. S. & Podile, A. R. (2012) Chitin binding proteins act synergistically with chitinases in *Serratia proteamaculans* 568. *PLoS One* **7**, e36714.
29. Vaaje-Kolstad, G., Bunæs, A. C., Mathiesen, G. & Eijsink, V. G. H. (2009) The chitinolytic system of *Lactococcus lactis* ssp. *lactis* comprises a nonprocessive chitinase and a chitin-binding protein that promotes the degradation of alpha- and beta-chitin. *FEBS J* **276**, 2402-2415.
30. Chen, S. L. & Wilson, D. B. (2007) Proteomic and transcriptomic analysis of extracellular proteins and mRNA levels in *Thermobifida fusca* grown on cellobiose and glucose. *J Bacteriol* **189**, 6260-6265.
31. Suzuki, K., Suzuki, M., Taiyoji, M., Nikaidou, N. & Watanabe, T. (1998) Chitin binding protein (CBP21) in the culture supernatant of *Serratia marcescens* 2170. *Biosci Biotechnol Biochem* **62**, 128-135.
32. Takasuka, T. E., Book, A. J., Lewin, G. R., Currie, C. R. & Fox, B. G. (2013) Aerobic deconstruction of cellulosic biomass by an insect-associated Streptomyces. *Scientific reports* **3**, 1030.
33. Hori, C., Gaskell, J., Igarashi, K., Samejima, M., Hibbett, D., Henrissat, B. & Cullen, D. (2013) Genomewide analysis of polysaccharides degrading enzymes in 11 white- and brown-rot Polyporales provides insight into mechanisms of wood decay. *Mycologia* **105**, 1412-1427.
34. Chater, K. F., Biro, S., Lee, K. J., Palmer, T. & Schrempf, H. (2010) The complex extracellular biology of Streptomyces. *FEMS Microbiol Rev* **34**, 171-198.
35. Kolbe, S., Fischer, S., Becirevic, A., Hinz, P. & Schrempf, H. (1998) The *Streptomyces reticuli* alpha-chitin-binding protein CHB2 and its gene. *Microbiology* **144**, 1291-1297.
36. Zeltins, A. & Schrempf, H. (1997) Specific interaction of the Streptomyces chitin-binding protein CHB1 with alpha-chitin--the role of individual tryptophan residues. *Eur J Biochem* **246**, 557-564.
37. Saito, A., Miyashita, K., Biukovic, G. & Schrempf, H. (2001) Characteristics of a *Streptomyces coelicolor* A3(2) extracellular protein targeting chitin and chitosan. *Appl Environ Microb* **67**, 1268-1273.
38. Book, A. J., Yennamalli, R. M., Takasuka, T. E., Currie, C. R., Phillips, G. N., Jr. & Fox, B. G. (2014) Evolution of substrate specificity in bacterial AA10 lytic polysaccharide monooxygenases. *Biotechnol Biofuels* **7**, 109.
39. Nakagawa, Y. S., Eijsink, V. G. H., Totani, K. & Vaaje-Kolstad, G. (2013) Conversion of alpha-chitin substrates with varying particle size and crystallinity reveals substrate preferences of the chitinases and lytic polysaccharide monooxygenase of *Serratia marcescens*. *J Agric Food Chem* **61**, 11061-11066.
40. Moser, F., Irwin, D., Chen, S. L. & Wilson, D. B. (2008) Regulation and characterization of Thermobifida fusca carbohydrate-binding module proteins E7 and E8. *Biotechnol Bioeng* **100**, 1066-1077.

41. Gardner, J. G., Crouch, L., Labourel, A., Forsberg, Z., Bukhman, Y. V., Vaaje-Kolstad, G., Gilbert, H. J. & Keating, D. H. (2014) Systems biology defines the biological significance of redox-active proteins during cellulose degradation in an aerobic bacterium. *Mol Microbiol*.

42. Igarashi, K., Uchihashi, T., Koivula, A., Wada, M., Kimura, S., Okamoto, T., Penttila, M., Ando, T. & Samejima, M. (2011) Traffic jams reduce hydrolytic efficiency of cellulase on cellulose surface. *Science* **333**, 1279-82.

43. Kurasin, M. & Valjamae, P. (2011) Processivity of cellobiohydrolases is limited by the substrate. *J Biol Chem* **286**, 169-177.

44. Jalak, J., Kurasin, M., Teugjas, H. & Valjamae, P. (2012) Endo-exo synergism in cellulose hydrolysis revisited. *J Biol Chem* **287**, 28802-15.

45. Igarashi, K., Uchihashi, T., Uchiyama, T., Sugimoto, H., Wada, M., Suzuki, K., Sakuda, S., Ando, T., Watanabe, T. & Samejima, M. (2014) Two-way traffic of glycoside hydrolase family 18 processive chitinases on crystalline chitin. *Nature comm* **5**, 3975.

46. Zakariassen, H., Aam, B. B., Horn, S. J., Vårum, K. M., Sørlie, M. & Eijsink, V. G. H. (2009) Aromatic residues in the catalytic center of chitinase a from *Serratia marcescens* affect processivity, enzyme activity, and biomass converting efficiency. *J Biol Chem* **284**, 10610-10617.

47. Suzuki, K., Sugawara, N., Suzuki, M., Uchiyama, T., Katouno, F., Nikaidou, N. & Watanabe, T. (2002) Chitinases A, B, and C1 of *Serratia marcescens* 2170 produced by recombinant Escherichia coli: enzymatic properties and synergism on chitin degradation. *Biosci Biotechnol Biochem* **66**, 1075-1083.

48. Horn, S. J., Sørbotten, A., Synstad, B., Sikorski, P., Sørlie, M., Vårum, K. M. & Eijsink, V. G. H. (2006) Endo/exo mechanism and processivity of family 18 chitinases produced by *Serratia marcescens*. *FEBS J* **273**, 491-503.

49. Horn, S. J., Sorlie, M., Varum, K. M., Valjamae, P. & Eijsink, V. G. (2012) Measuring processivity. *Methods Enzymol* **510**, 69-95.

50. Horn, S. J., Sikorski, P., Cederkvist, J. B., Vaaje-Kolstad, G., Sørlie, M., Synstad, B., Vriend, G., Vårum, K. M. & Eijsink, V. G. H. (2006) Costs and benefits of processivity in enzymatic degradation of recalcitrant polysaccharides. *Proc Natl Acad Sci U S A* **103**, 18089-18094.

51. Fox, J. M., Levine, S. E., Clark, D. S. & Blanch, H. W. (2012) Initial- and processive-cut products reveal cellobiohydrolase rate limitations and the role of companion enzymes. *Biochemistry* **51**, 442-52.

52. Brurberg, M. B., Eijsink, V. G. H. & Nes, I. F. (1994) Characterization of a chitinase gene (chiA) from *Serratia marcescens* BJL200 and one-step purification of the gene product. *FEMS Microbiol Lett* **124**, 399-404.

53. Brurberg, M. B., Eijsink, V. G. H., Haandrikman, A. J., Venema, G. & Nes, I. F. (1995) Chitinase B from *Serratia marcescens* BJL200 is exported to the periplasm without processing. *Microbiology* **141**, 123-131.

54. Synstad, B., Vaaje-Kolstad, G., Cederkvist, H., Saua, S. F., Horn, S. J., Eijsink, V. G. H. & Sørlie, M. (2008) Expression and characterization of endochitinase C from *Serratia marcescens*

BJL200 and its purification by a one-step general chitinase purification method. *Biosci Biotechnol Biochem* **72**, 715-723.

55. Fan, Y., Saito, T. & Isogai, A. (2008) Preparation of chitin nanofibers from squid pen beta-chitin by simple mechanical treatment under acid conditions. *Biomacromolecules* **9**, 1919-1923.

56. Heuts, D. P., Winter, R. T., Damsma, G. E., Janssen, D. B. & Fraaije, M. W. (2008) The role of double covalent flavin binding in chito-oligosaccharide oxidase from *Fusarium graminearum*. *Biochem J* **413**, 175-183.

57. Arnold, K., Bordoli, L., Kopp, J. & Schwede, T. (2006) The SWISS-MODEL workspace: a web-based environment for protein structure homology modelling. *Bioinformatics* **22**, 195-201.

58. Dereeper, A., Guignon, V., Blanc, G., Audic, S., Buffet, S., Chevenet, F., Dufayard, J. F., Guindon, S., Lefort, V., Lescot, M., Claverie, J. M. & Gascuel, O. (2008) Phylogeny.fr: robust phylogenetic analysis for the non-specialist. *Nucleic Acids Res* **36**, W465-W469.

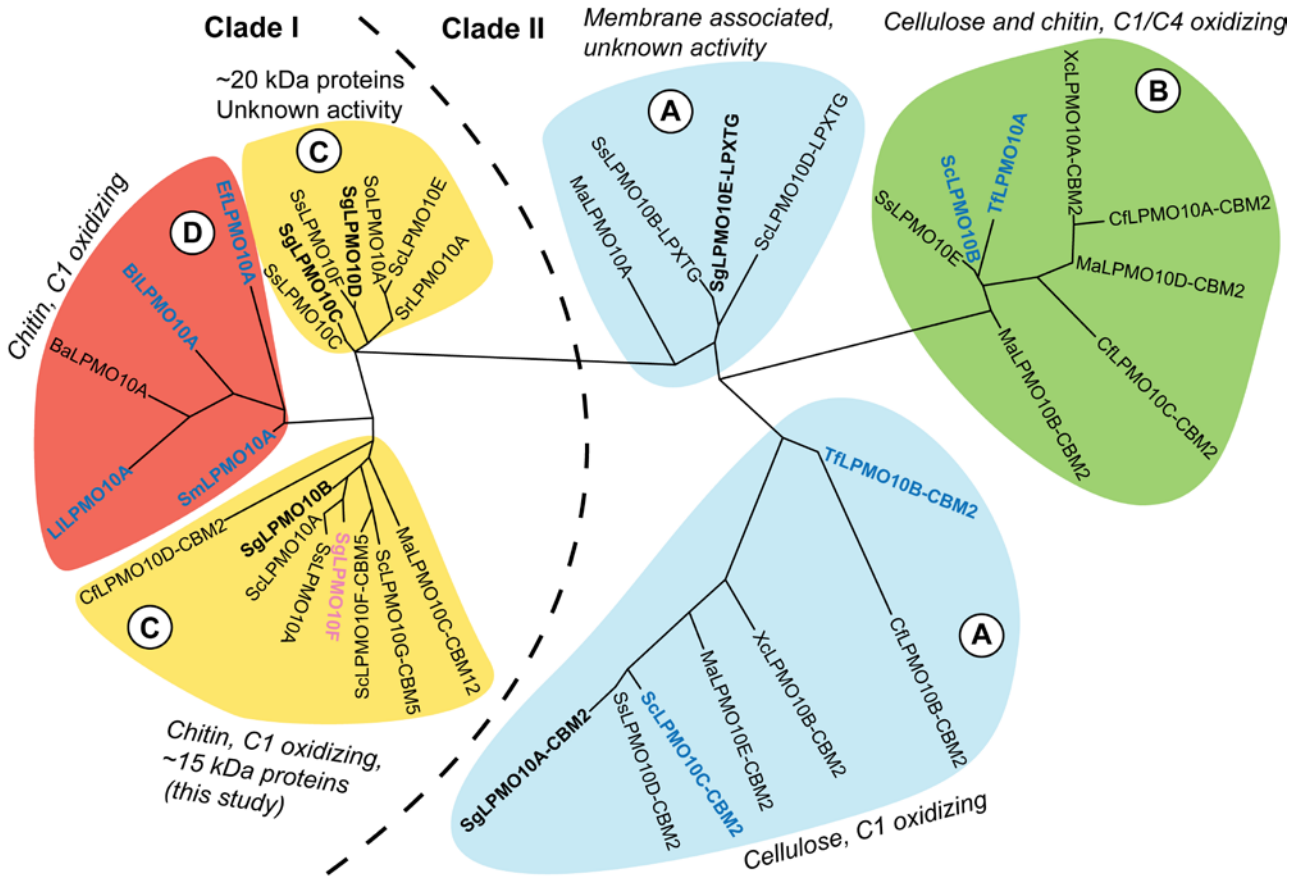
Clade I
Clade II
Membrane associated, unknown activity
Cellulose and chitin, C1/C4 oxidizing
~20 kDa proteins
Unknown activity
Chitin, C1 oxidizing
Chitin, C1 oxidizing, ~15 kDa proteins (this study)
Cellulose, C1 oxidizing
A
B
C
D
SsLPMO10B-LPXTG
MaLPMO10A
SgLPMO10E-LPXTG
ScLPMO10D-LPXTG
XcLPMO10A-CBM2
TfLPMO10A
ScLPMO10B
SsLPMO10E
CfLPMO10A-CBM2
MaLPMO10D-CBM2
MaLPMO10B-CBM2
CfLPMO10C-CBM2
EfLPMO10A
BlLPMO10A
BaLPMO10A
LlLPMO10A
SmLPMO10A
SsLPMO10F
SgLPMO10D
SgLPMO10C
SsLPMO10C
SoLPMO10A
ScLPMO10E
SrLPMO10A
CfLPMO10D-CBM2
SgLPMO10B
ScLPMO10A
SsLPMO10A
ScLPMO10F
ScLPMO10F-CBM5
ScLPMO10G-CBM5
MaLPMO10C-CBM12
TfLPMO10B-CBM2
CfLPMO10B-CBM2
XcLPMO10B-CBM2
MaLPMO10E-CBM2
ScLPMO10C-CBM2
SsLPMO10D-CBM2
SgLPMO10A-CBM2

673

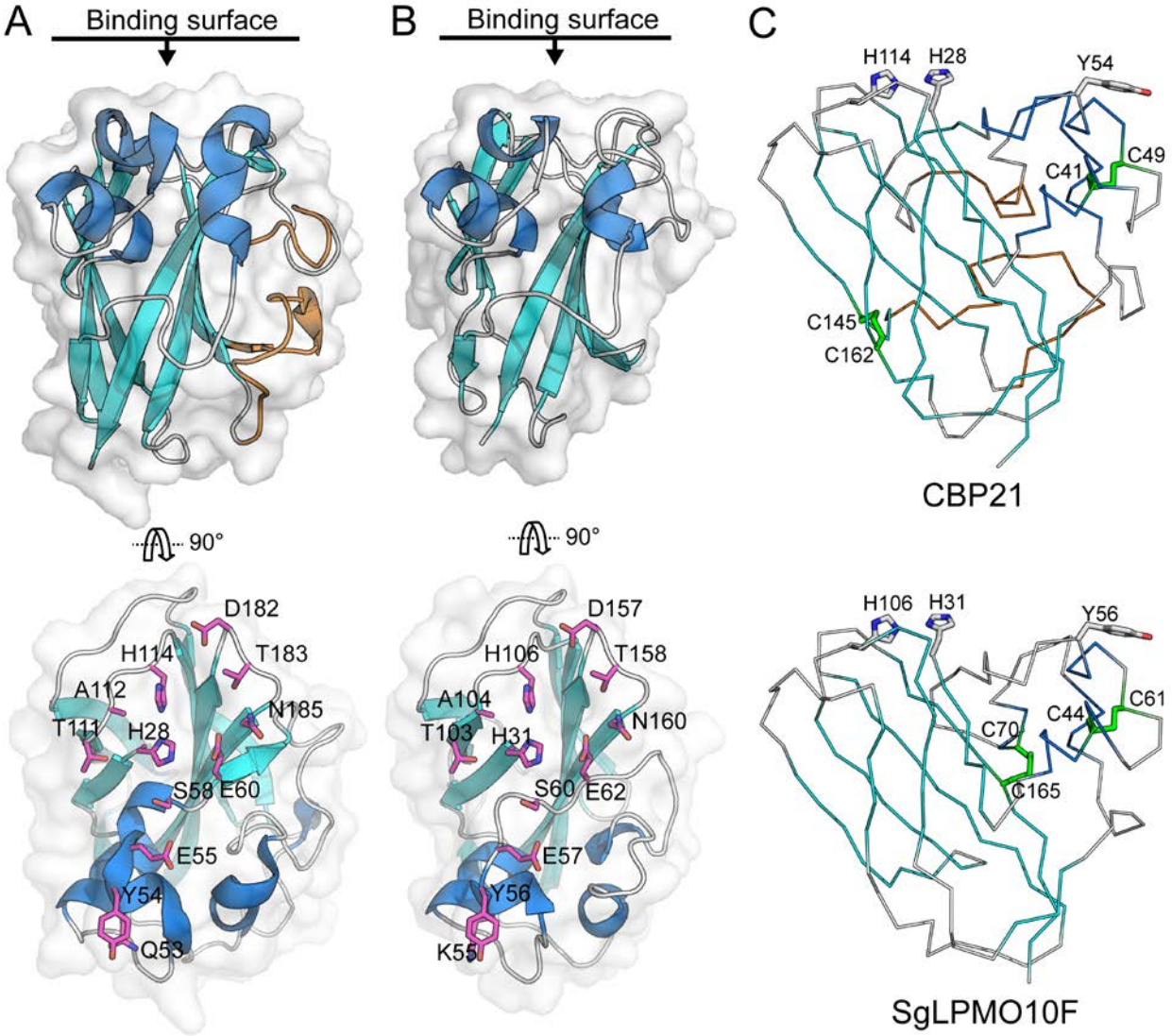
A
Binding surface
B
Binding surface
C
H114
H28
Y54
C49
C41
C145
C162
CBP21
90°
90°
D182
H114
T183
A112
N185
T111
H28
S58
E60
E55
Y54
Q53
D157
H106
T158
A104
N160
T103
H31
S60
E62
E57
Y56
K55
H106
H31
Y56
C61
C44
C70
C165
SgLPMO10F

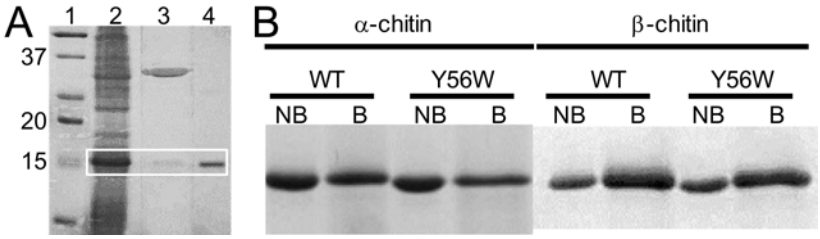
A
1
2
3
4
37
20
15
B
α-chitin
β-chitin
WT
Y56W
WT
Y56W
NB
B
NB
B
NB
B
NB
B

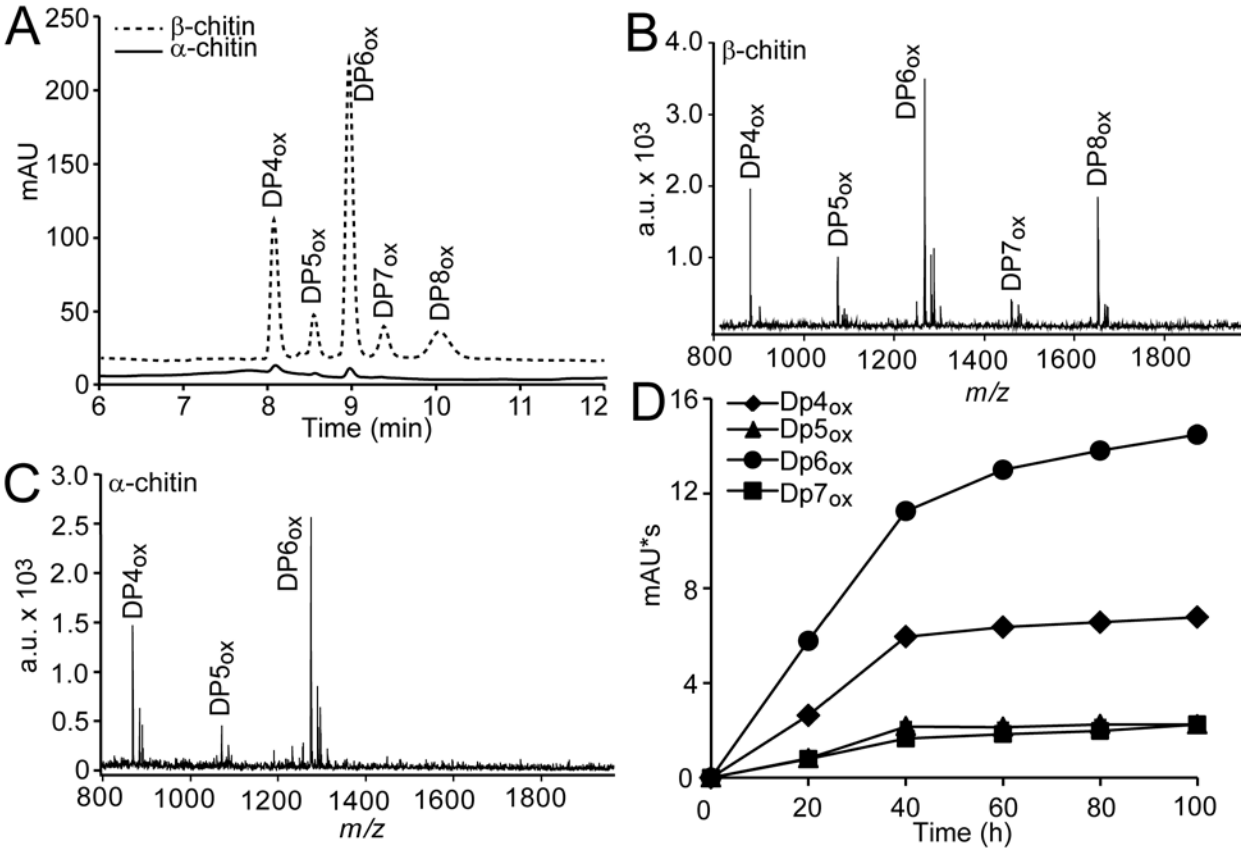
A
β-chitin
α-chitin
mAU
Time (min)
DP4ox
DP5ox
DP6ox
DP7ox
DP8ox
B
β-chitin
a.u. x 103
m/z
C
α-chitin
a.u. x 103
m/z
D
Dp4ox
Dp5ox
Dp6ox
Dp7ox
mAU*s
Time (h)

676

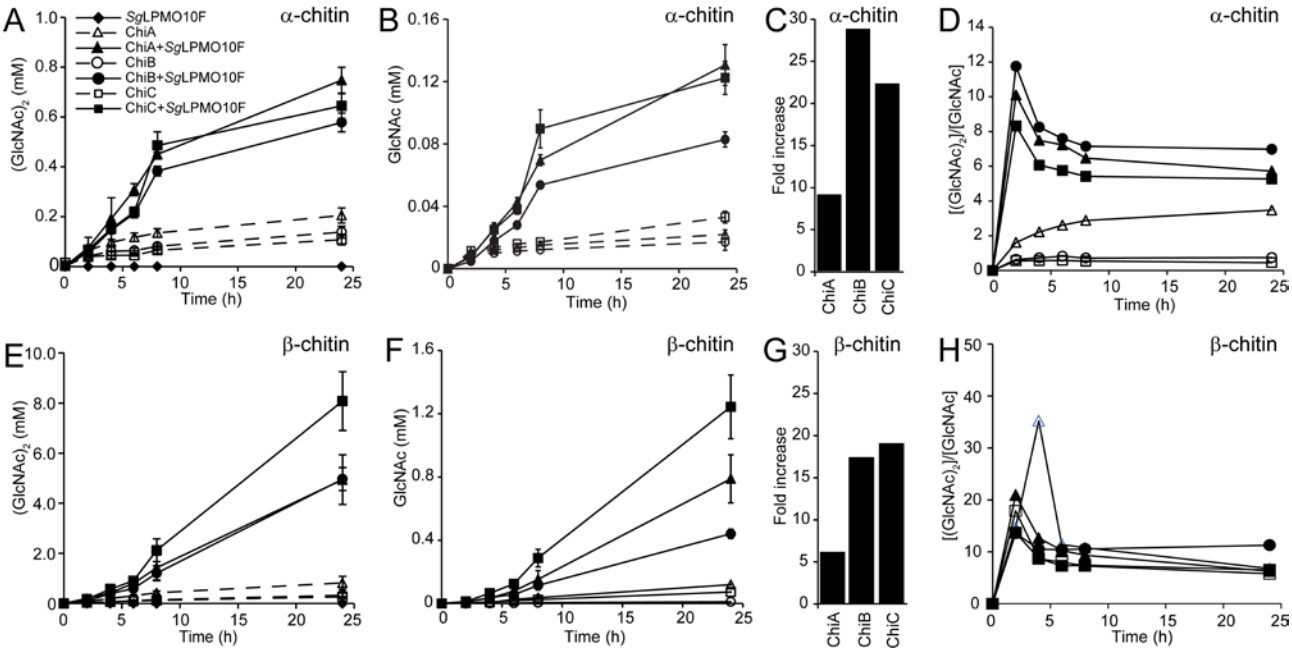
A
α-chitin
SgLPMO10F
ChiA
ChiA+SgLPMO10F
ChiB
ChiB+SgLPMO10F
ChiC
ChiC+SgLPMO10F
(GlcNAc)2 (mM)
Time (h)
B
α-chitin
GlcNAc (mM)
Time (h)
C
α-chitin
Fold increase
ChiA
ChiB
ChiC
D
α-chitin
[(GlcNAc)2]/[GlcNAc]
Time (h)
E
β-chitin
(GlcNAc)2 (mM)
Time (h)
F
β-chitin
GlcNAc (mM)
Time (h)
G
β-chitin
Fold increase
ChiA
ChiB
ChiC
H
β-chitin
[(GlcNAc)2]/[GlcNAc]
Time (h)

677

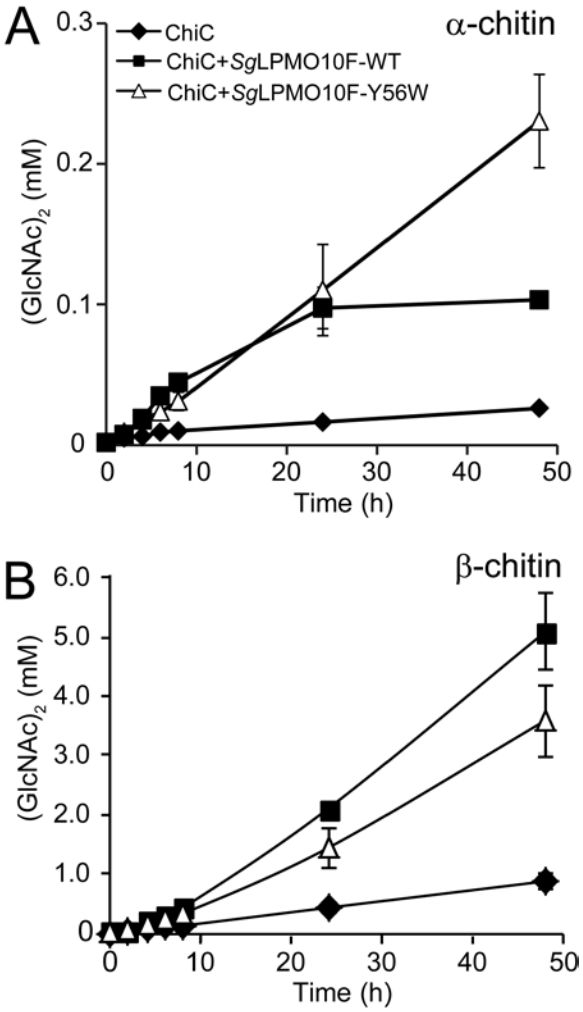
A
α-chitin
ChiC
ChiC+SgLPMO10F-WT
ChiC+SgLPMO10F-Y56W
(GlcNAc)2 (mM)
0.3
0.2
0.1
0
0
10
20
30
40
50
Time (h)
B
β-chitin
(GlcNAc)2 (mM)
6.0
5.0
4.0
3.0
2.0
1.0
0
0
10
20
30
40
50
Time (h)

678